Photonic Sensors (2011) Vol. 1, No. 1: 62−71

DOI: 10.1007/s13320-010-0014-z **Photonic Sensors**

Review

Recent Developments in Fiber Optic Spectral White-Light Interferometry

Yi JIANG and Wenhui DING

School of Optoelectronics, Beijing Institute of Technology, Beijing,100081, China

*Corresponding author: Yi JIANG E-mail: bitjy@bit.edu.cn

Abstract: Recent developments in spectral white-light interferometry (WLI) are reviewed. Firstly, the techniques for obtaining optical spectrum are introduced. Secondly, some novel measurement techniques are reviewed, including the improved peak-to-peak WLI, improved wavelength-tracking WLI, Fourier transform WLI, and 3 × 3 coupler based WLI. Furthermore, a hybrid measurement for the intensity-type sensors, interferometric sensors, and fiber Bragg grating sensors is achieved. It is shown that these developments have assisted in the progress of WLI.

Keywords: Optical fiber sensors, white-light interferometry, optical path difference, fiber Fabry-Perot tunable filter, extrinsic Fabry-Perot interferometer

1. Introduction

Fiber optic sensors possess numerous advantages over conventional electrical sensors, such as small size, light weight, high sensitivity, immunity to electromagnetic interference, and capability of multiplexing [1]. In particular, the interferometric sensor has developed into one of the primary fiber optic sensors. The output signal from an interferometer is nonlinear for a linear input, thus, homodyne and heterodyne demodulation techniques are proposed to recover the phase change caused by a measurand. However, these two techniques are generally used to measure a dynamic perturbation, such as vibration and sound, because neither the homodyne nor the heterodyne technique can determine the absolute optical path difference (OPD) of an interferometer.

Fiber optic white-light interferometry (WLI) is widely used to interrogate the absolute OPD of an interferometer. WLI possesses a considerable advantage with regard to the ability to provide absolute and unambiguous measurements, compared with homodyne and heterodyne interferometry, and can be used to measure a static measurand, such as temperature, strain, and pressure, etc. Scanning WLI and spectral WLI are two major kinds of white-light interferometry. Scanning WLI requires a wide-band source and a receiving interferometer. Recovering the OPD of the sensing interferometer requires the OPD of the local receiving interferometer to be scanned, resulting in a white-light interferometric fringe [2−4]. The disadvantages of the technique include large system size, low mechanical stability, and relatively low efficiency. Thus, it is difficult for the scanning WLI to be used in an engineering application. Spectral WLI is based on the detection of the optical spectrum of the sensing interferometer, and the absolute OPD can be interrogated by analyzing the spectrum [5−6]. Spectral WLI has no mechanical scanning system, and posses properties of small size, solidity, and high efficiency. Two

Received: 20 September 2010 / Revised version: 28 September 2010

wavelengths are generally the wavelengths of two adjacent peaks in a white-light optical spectrum. Although many schemes are available to recover the OPD from a white-light spectrum, there are two problems for the spectral WLI: one is that the commercialized optical spectral analyzer (OSA) is cumbersome in dealing with the data and unsuitable for instrumentation; the other is the difficulty in determining the peak position precisely in a white-light optical spectrum, because the optical-spectrum curve is in sine distribution. These are proved to be two major limitations in the applications for the spectral WLI. In the paper, recent developments toward solving these two problems are reviewed. It is shown that these improvements have assisted in overcoming the limitations of WLI and promote the progress of the technique.

2. Collection of a white-light optical spectrum

There are two methods to obtain the white-light optical spectrum of an interferometer: one method is to use a broadband light source and to detect the output light with an OSA; the other method is to illuminate an interferometer with a wavelength-scanning light source and to detect the output light with a photoelectric diode. The second method is characteristic of small size and low cost. It needs a fiber Fabry-Perot tunable filter (FFP-TF) or an FFP-TF-based scanning fiber laser [7−8]. Driven by a piezoelectric transducer (PZT), the FFP-TF exhibits a nonlinear hysteresis behavior and poor repeatability. These problems make it difficult to precisely determine the scanning wavelength. A method to obtain the optical spectrum of an interferometer by using a wavelength calibration technique is demonstrated, in which a fiber optic etalon is used to calibrate the nonlinear wavelength change caused by an FFP-TF, and good wavelength repeatability is achieved [9].

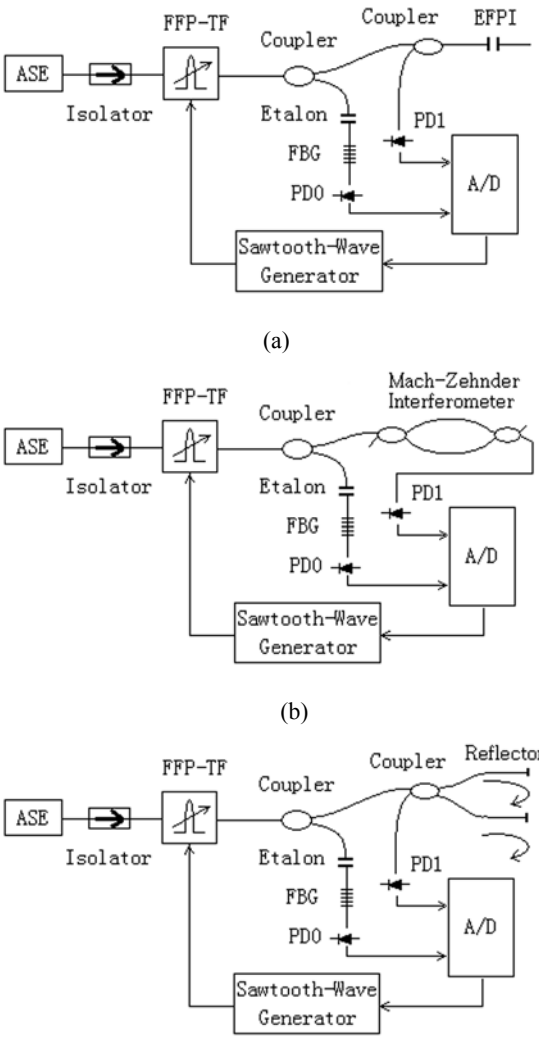

Fig. 1 Configurations of white-light interferometry: (a) extrinsic Fabry-Perot interferometer, (b) Mach-Zehnder interferometer, and (c) Michelson interferometer.

Configurations for obtaining the spectra of three interferometers are all shown in Fig. 1. An amplified spontaneous emission (ASE) source is used as a broadband source to illuminate an FFP-TF. A sawtooth-wave generator is triggered by a computer to produce a linear-scanning voltage and the sawtooth-wave voltage is used to drive the FFP-TF. The wavelength-scanning light is divided into two beams by a coupler. One beam is injected into the sensing interferometer and the interferometric output is detected by a photo-diode, PD1. This beam is

used to detect the white-light optical spectrum of the sensing interferometer. The other beam is injected into an etalon combined with a fiber Bragg grating (FBG) and the transmission light is detected by another photo-diode, PD0. This beam is used to calibrate the output wavelength of FFP-TF. After the spectra of the sensing interferometer and etalon are sampled into the computer, the wavelength calibration is performed to change the spectrum of the interferometer from sampling sequence to wavelength sequence by using the spectrum of the etalon.

Figures 2 (a) and 2 (b) demonstrate the white-light optical spectrum obtained by an OSA and an FFP-TF, respectively, in which a Mach-Zehnder interferometer is under test. Two white-light optical spectra obtained by the two methods are the same. The technique presented in [9] has advantages over an OSA, such as small size, solidity, low cost, and high resolution. It is preferable for instrumentation.

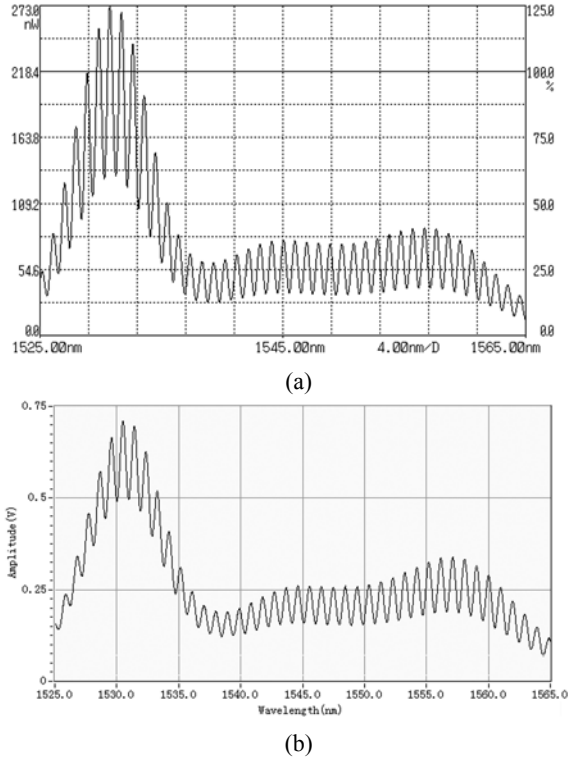

Fig. 2 White-light optical spectrum obtained by (a) an OSA AQ6317C and (b) scanning the FFP-TF.

3. Spectral WLI

After the white-light optical spectrum is obtained, we can retrieve the absolute OPD by analyzing the spectrum curve. Several demodulation algorithms to retrieve the OPD of an interferometer from the optical spectrum have been proposed. The peak-to-peak method, which detects the wavelength difference of two adjacent fringe peaks, is the main technique to measure the OPD [5−6]. With wavelength scanning from λ_1 to λ_2, an interferometer has a phase change of φ because there is an OPD. The relationship between φ and OPD is given by

$$\varphi = \frac{2\pi(\lambda_2 - \lambda_1)}{\lambda_1 \lambda_2} \cdot D \tag{1}$$

where D is OPD of an interferometer. The OPD is obtained by the peak-to-peak method when λ_1 and λ_2 are the wavelengths of two adjacent peaks on the spectrum, namely

$$D = \frac{\lambda_1 \lambda_2}{\lambda_2 - \lambda_1}. \tag{2}$$

Because the curve of the optical spectrum is in sine distribution, there is a large uncertainty in determining the peak position, which limits the wavelength discrimination for the peak-to-peak method. For a short cavity length, a linear or quadrature operation is proved to be considerable for the high sensitivity, but the measurement range is limited in $\lambda/2$ [10, 11]. Another popular method is the fast Fourier transform (FFT) based frequency technique, which transforms the signal from a wavelength domain to a cavity length domain [7, 12−13]. With this method, the peak position of the Fourier spectrum is detected to calculate the OPD. However, the resolution is very low. Our experimental results show that, for an OPD of 1800 μm, one hertz on the frequency spectrum after FFT represents a cavity length of 29 μm [9].

In the later part of this section, we will review the recent progress in retrieving the absolute OPD, especially focusing on the phase demodulation based techniques.

3.1 Improved peak-to-peak WLI

Reference [9] demonstrates an improved technique to interrogate the absolute cavity length of an extrinsic Fabry-Perot interferometer (EFPI) by peak-to-peak method. The improved method is realized by the following steps:

1) The positions of all apexes are calculated with the conventional peak detection technique and all wavelength spacings between two adjacent apexes are measured.

2) Linear fitting is carried out by using the wavelength spacing and a linear fitting equation describing the relationship between the wavelength spacing $\Delta\lambda_{MM}$ and wavelength λ is obtained.

3) The wavelength spacing $\Delta\lambda_{MM}$ with a 2π phase shift at 1550 nm is calculated with the fitting equation.

4) The OPD is calculated by using the calculated wavelength spacing.

The uncertainty in measuring the peak wavelength can be reduced by using linear fitting arithmetic. An experimental linear fitting curve is shown in Fig. 3. We can precisely calculate the wavelength of any apex according to this equation. The improved technique was compared with the conventional peak-to-peak detection technique. The cavity length was fixed at 2511 μm and the measurement was performed 322 times. For the improved peak-to-peak method, the variation is limited to ±1 μm. For the conventional peak-to-peak method, the variation is ±25 μm. The resolution is improved by a factor of 25 times.

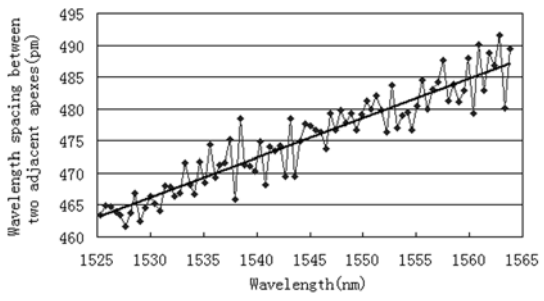

Fig. 3 Wavelength spacing between two adjacent apexes from 1525 nm to 1565 nm; the straight line is a linear fitting line.

3.2 Improved wavelength-tracking WLI

The wavelength-tracking method is realized by measuring the wavelength shift of one peak in the spectrum. This method has a higher resolution than the peak-to-peak method; but the dynamic range is only $\lambda/2$, where λ is the spectrum position of the monitored band under no external perturbation [14]. The wavelength-tracking method does not measure the absolute OPD, it only monitors the wavelength shift of a interference fringe peak.

References [14] and [15] demonstrate an improved wavelength-tracking method to interrogate the OPD. The OPD can be calculated with high resolution by using the equation

$$D = \text{Integer}[\frac{\lambda_2}{(\lambda_2 - \lambda_1)}] \cdot \lambda_1 . \qquad (3)$$

This method can measure the absolute OPD with the same resolution as the conventional wavelength-tracking method, but there is no limitation to the dynamic range. The measurement resolution is only limited by the variation in detecting the peak wavelengths in a white-light optical spectrum.

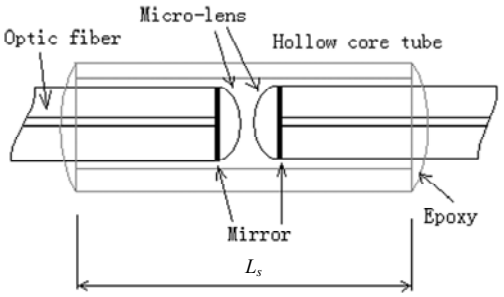

Fig. 4 Illustration of a micro-lens EFPI.

To reach a high measurement resolution, a high-finesse interferometer, such as a high-finesse fiber Fabry-Perot interferometer (FFPI), is desired as a sensor. We have presented a micro-lens EFPI resonator which is easy to construct at a low cost [16]. The resonator is suitable as a high-finesse sensor and its finesse is much greater than that of an EFPI with two plain mirrors. The configuration of the micro-lens Fabry-Perot interferometer is illustrated in Fig. 4. The transmission spectrum of the micro-lens EFPI is shown in Fig. 5. The EFPI

has a free spectrum range (FSR) of 14.5 nm, a bandwidth of 0.23 nm, and thus a finesse of 63.

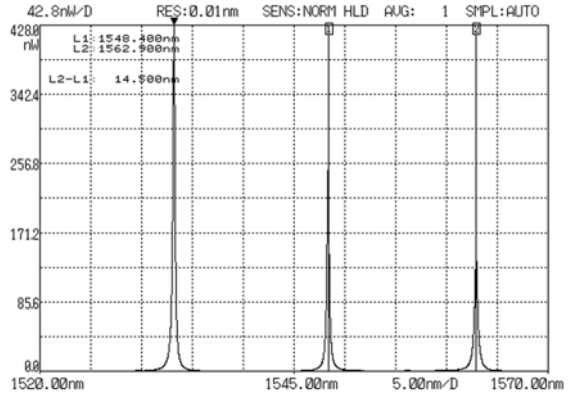

Fig. 5 Transmission spectrum of a micro-lens EFPI.

The improved wavelength-tracking method was used to interrogate the high-finesse interferometric sensor. The white-light spectrum was obtained by the technique described in Section 2. An optical cavity length of 75,367 nm with a variation of ±1 nm was obtained by using the improved method, as shown in Fig. 6 when a continuous test was carried out 1400 times without any artificial interference. Figure 6 shows a high measurement resolution is achieved.

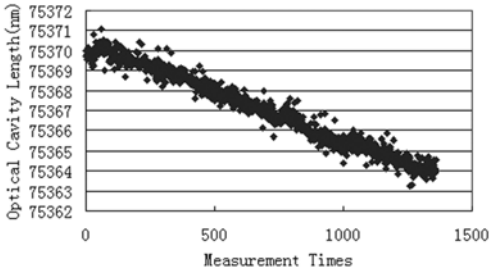

Fig. 6 A continuous test.

3.3 Fourier transform WLI

We have presented a phase recovering technique to interrogate the OPD of an interferometer, namely Fourier transform interferometry [17]. With this technique, firstly the optical spectrum is Fourier transformed. The main component is filtered and inverse Fourier transformed. Then we calculate a complex logarithm of the product. We can obtain the phase change of the fringe signal in the imaginary part, which is caused by scanning wavelength. Thus, the absolute OPD can be calculated by using the phase change.

The system of interrogating an EFPI is shown in Fig. 1 (a). The obtained optical spectrum is shown in Fig. 7(a). The Fourier spectrum is shown in Fig. 7 (b). The spectrum was filtered and inverse Fourier transformed, as shown in Fig. 7 (c). Then we obtained the imaginary part and the unwrapped phase. The cavity length was calculated to be 2298.7 μm, which was in agreement with the actual value.

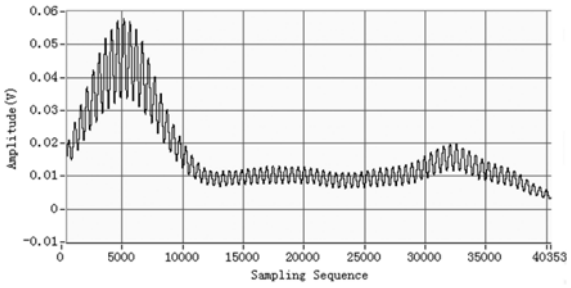

(a)

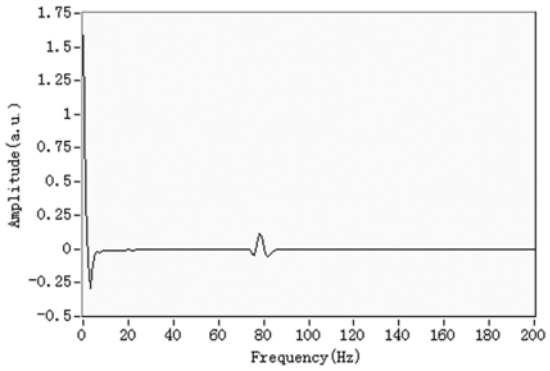

(b)

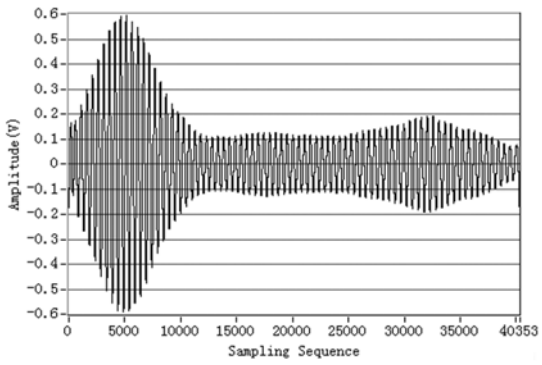

(c)

Fig. 7 (a) The scanned optical spectrum with wavelength interval of 1 pm, (b) the Fourier spectrum of the optical spectrum, and (c) the obtained signal after the signal in (a) is Fourier transformed, filtered, and inverse transformed. In (a) and (c), the sampling interval is 1 pm and the *x*-coordinate in the two figures is the wavelength from 1525.139 nm to 1565.491 nm.

3.4 Phase comparing WLI

To remove the common interference caused by the environmental interference and the instability of interrogator, and to increase the measurement resolution, a reference interferometer can be introduced into a WLI system. A Fourier transform phase comparator is developed to calculate the phase difference caused by the scanning wavelength and the OPD difference between two interferometers can be obtained [18]. The system for interrogating an EFPI strain sensor with another compensating EFPI is shown in Fig. 8. Two EFPIs should have similar cavity length and sensor length, in order to undergo the same environmental change. Two EFPIs are connected to the interrogator by a coupler array. EFPI 1# is used as a strain sensor and EFPI 2# is used as a compensator.

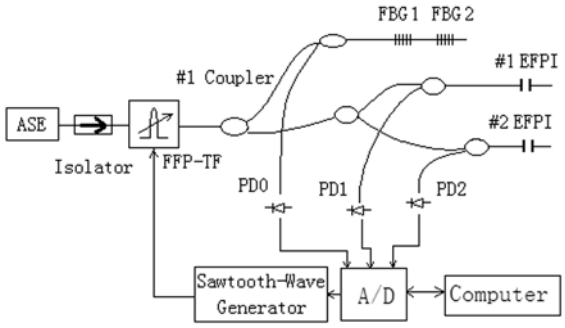

Fig. 8 Experimental setup of the phase comparing WLI.

In the measurement system, the reference EFPI is used to sense the common interferences caused by environmental changes and the uncertainty of the scanning wavelength, except the strain. The sensing EFPI is attached to the structure. Thus, the common interferences can be removed and the cavity length difference Δd between the two EFPIs can be measured with high resolution.

The cavity length difference Δd between the two EFPIs was measured and the results are shown in Fig. 9, in which the variation is only ±0.35 nm. We also found in Fig. 9 that the cavity length difference had no response to temperature change. We owe this advantage to the presence of the compensating EFPI, which has the same dimension and properties as that of the sensing EFPI.

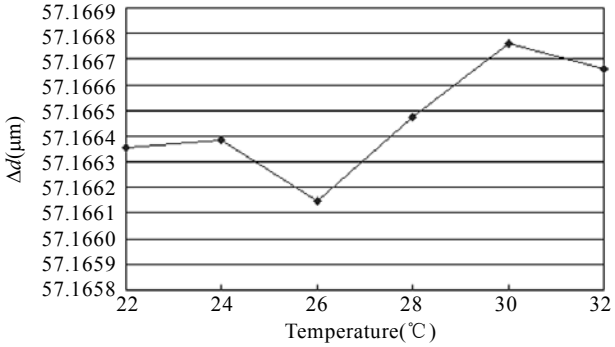

Fig. 9 Experimental result when temperature rises from 22 ℃ to 32 ℃.

3.5 Multiplexing based on Fourier transform WLI

Fourier transform WLI can be easily used to multiplex several interferometers [19]. In Fig. 1 (a), two EFPIs, with cavity lengths of 1007 μm and 3000 μm respectively, are parallelly connected to the interrogator by a 1 × 2 coupler. The sampled synthetic optical spectrum is shown in Fig. 10 (a). The white-light optical spectrum is then Fourier transformed and the Fourier spectrum is shown in Fig. 10 (b). There are two carrier frequencies in the frequency domain: one is 34 Hz and the other is 102 Hz. The carrier frequency of 34 Hz corresponds to a cavity length of 1007 μm and the carrier frequency of 102 Hz corresponds to a cavity length of 3000 μm. Two carrier-frequency components in the frequency domain are filtered respectively by two filters and we obtain two spectra. Then the two spectra are inverse Fourier transformed respectively and we obtain two analytic signals. When scanning the wavelength from 1524.7 nm to 1565.3 nm, the phase changes of two fringes are measured using the analytic signals. Then the cavity length was calculated to be 1007.0 μm for EFPI #1 and 3005.4 μm for EFPI #2. Two EFPIs are all interrogated and

there is no cross talk between the two multiplexed EFPIs.

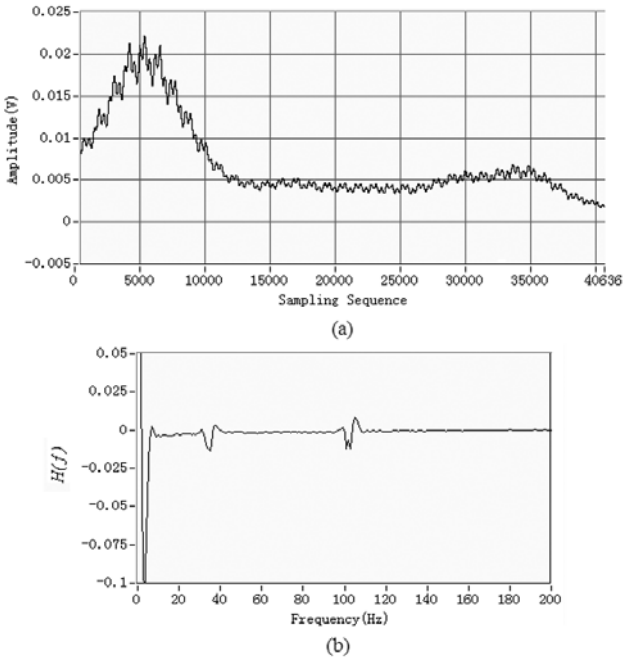

Fig. 10 (a) The white-light optical spectrum of two EFPIs and (b) the Fourier spectrum of the optical spectrum.

3.6 3 × 3 coupler based WLI

In Fourier transform WLI, the Fourier transform and inverse Fourier transform will take much time, which limits its application in a high-rate measurement. We propose another method to retrieve the phase change caused by scanning wavelength by using a 3 × 3 coupler-based interferometer [20]. Figure 11 shows the experimental schematic diagram of a 3 × 3 coupler based WLI measurement system. Illuminated with a wavelength-scanning source, the unbalanced Mach-Zehnder interferometer behaves as a spectral filter with a cosine transfer function. The phase change caused by scanning wavelength can be directly obtained by using a 3 × 3 coupler-based interferometer. A 3 × 3 coupler, which has the same power transfer ratios at the output ports, possesses a natural ability to provide a 120° phase-shifted signal without an active component [21−23].

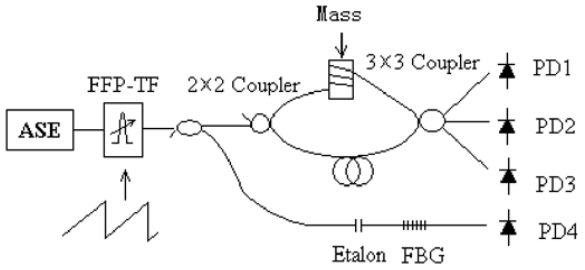

Fig. 11 Schematic diagram of a 3 × 3 coupler-based WLI.

One of the three sampled white-light optical spectra of the interferometer and the spectrum of the etalon are shown in Figs. 12 (a) and 12 (b), respectively. With wavelength scanning from 1525.649 nm to 1563.861 nm, the induced phase change can be demodulated with a software demodulator by using three white-light optical spectra [21−23] and the demodulated phase change is shown in Fig. 13 (a). In the meantime, Fourier transform WLT is also used to calculate the phase change and the result is shown in Fig. 13 (b). Figures 13 (a) and 13 (b) have the same phase change when scanning the wavelength, proving that this method reaches the same result as that obtained with Fourier transform WLI. Thus, the path difference of the interferometer can be calculated to be 1358.8 μm. With this technique, a high resolution can be achieved for the measurement of static parameters, such as pressure, weight, strain, and so on.

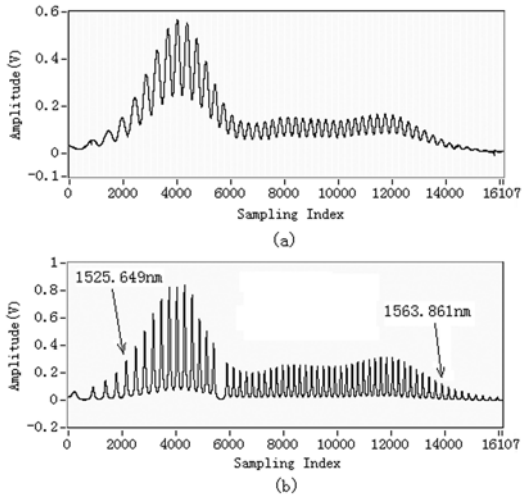

Fig. 12 Sampled datum arrays when scanning the FFP-TF: (a) white-light spectrum and (b) spectrum of the etalon.

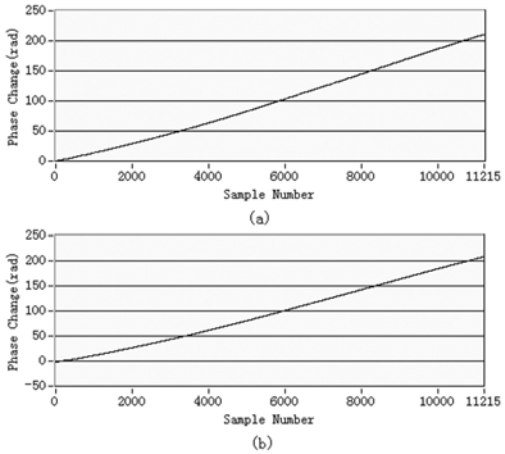

Fig. 13 Phase changes when scanning the wavelength from 1525.649 nm to 1563.861 nm: (a) obtained by 3 × 3 coupler based interferometry and (b) obtained by Fourier transform WLI.

4. Hybrid interrogation

With the development of fiber optic sensing technology, hybrid demodulation for different types of sensors has attracted intensive interest from researchers. A hybrid interrogation system for an intensity-type sensor, fiber Bragg grating, and extrinsic Fabry-Perot interferometer is demonstrated [24]. Figure 14 shows the concept of the demodulation system. One EFPI, one intensity-type sensor, and two FBGs are interrogated in the system. Three types of sensors occupy different wavelength ranges from 1524 nm to 1563 nm and all sensors are wavelength-division multiplexed and interrogated in one demodulation system.

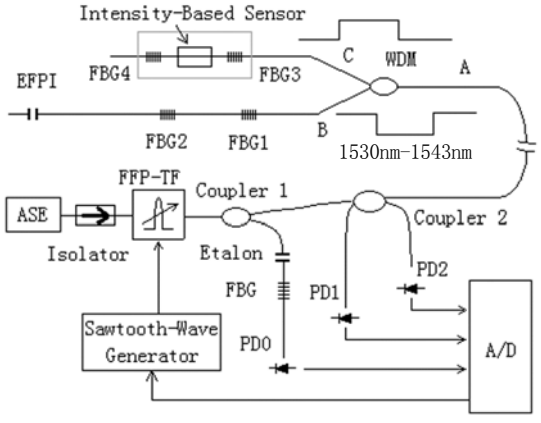

Fig. 14 Hybrid demodulation system for an intensity-based sensor, an EFPI, and two FBGs.

The EFPI has a maximum reflectivity of 8% because the reflectivity of fiber end is less than 4% and the reflectivity of FBG is greater than 70%. Thus, with a threshold, the peak of an FBG can be discriminated from the background, which is a sine curve caused by EFPI. The absolute wavelength of an FBG can be calculated by referencing the spectrum peaks of the etalon. To retrieve the absolute cavity length of an EFPI, Fourier transform WLI is utilized, with which two peaks on the spectrum of the etalon are selected to act as the start wavelength and the end wavelength when scanning the wavelength. The loss of the intensity-modulated sensor is interrogated by comparing the reflectivity of two FBGs which sandwich the intensity-modulated sensor [25]. However, if the intensity-type sensor with an FBG on either side is connected in series with the EFPI, the phase change of the EFPI will affect the spectrum heights of the two FBGs, interfering with the measurement of the intensity-modulated sensor. Besides, the intensity-type sensor will produce great loss, which will weaken the interference fringe of the EFPI, making it difficult to interrogate. This problem can be solved by introducing a wavelength division multiplexer (WDM) which has a transmission band from 1530 nm to 1543 nm. The WDM is connected to the system as shown in Fig. 14 with the transmission port connected to the intensity-type sensor and the reflection port connected to the FBG and EFPI sensors. Thus, the wavelength range used for interrogating FBGs is 1524 nm to 1529 nm, while a range of 1530 nm to 1543 nm is used for interrogating an intensity-type sensor and a range of 1545 nm to 1563 nm is used for interrogating an EFPI.

While the FFP-TF is scanning the wavelength, the outputs detected by three photo-diodes are sampled at the same time. After wavelength calibration, the optical spectrum of sensors is divided by the spectrum of the ASE. The normalized spectrum is shown in Fig. 15. Thus, the reflectivity

ratio of two FBGs around the intensity-type sensor is independent of the profile of the light source. Three types of sensors are all interrogated.

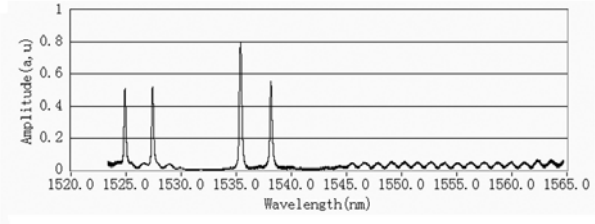

Fig. 15 Optical spectrum in which the spectrum profile of ASE source is removed.

5. Conclusions

The recent progress in spectral WLI has been summarized and reviewed in this paper. A number of novel techniques have been presented and demonstrated to retrieve the absolute OPD of an interferometer. A wavelength scanning method based on FFP-TF is demonstrated to obtain the optical spectrum of an interferometer. This method has advantages of small size, solidity, low cost, and high resolution, and is preferable for instrumentation. A linear fitting arithmetic is developed in the peak-to-peak WLI to overcome the uncertainty in determining the peak wavelength. For a high-finesse interferometer, an improved wavelength-tracking WLI is developed to precisely measure the OPD. Fourier transform WLI is proposed to retrieve the absolute OPD by measuring the phase change caused by the scanning wavelength. The multiplexing technique is also demonstrated. To remove the common perturbation, a phase comparator is developed to calculate the phase difference between two interferometers. To achieve high-speed and automatic measurement, a 3 × 3 coupler based WLI is proposed to measure the phase change caused by scanning wavelength. The spectrum based technique can be used to hybrid interrogate the intensity-type sensor, interferometric sensor, and wavelength-modulated sensor (i.e., FBG). With the presented techniques, we believe that WLI can measure the absolute OPD with the high resolution that heterodyne and homodyne techniques reach, and the effort promotes the progress in spectral WLI.

Acknowledgement

This work was supported by the National Natural Scientific Foundation of China (51075037), the Program for New Century Excellent Talents (NCET) at the University of China and Chinese 863 Project (2008AA04Z406).

References

[1] B. Lee, “Review of the present status of optical fiber sensors,” *Optical Fiber Technology*, vol. 9, no. 2, pp. 57−79, 2003.

[2] F. Depiereux, N. Konig, T. Pfeifer, and R. Schmitt, “Fiber-based white-light interferometer with improved sensor tips and stepped mirror,” *IEEE Transactions on Instrumentation and Measurement*, vol. 56, no. 6, pp. 2279−2283, 2007.

[3] Y. Chen and H.F. Taylor, “Multiplexed fiber Fabry-Perot temperature sensor system using white-light interferometry,” *Optics Letters*, vol. 27, no. 11, pp. 903−905, 2002.

[4] L. B. Yuan, L. M. Zhou, W. Jin, and C. C. Chan, “Recent progress of white light interferometric fiber optic strain sensing techniques,” *Review of Scientific Instruments*, vol. 71, no. 12, pp. 4648−4654, 2000.

[5] V. Bhatia, K. A. Murphy, R. O. Claus, T. A. Tran, and J. A. Greene, “Recent developments in optical-fiber-based extrinsic Fabry-Perot interferometric strain sensing technology,” *Smart Material and Structures*, vol. 4, no. 4, pp. 246−251, 1995.

[6] J. S. Leung and A. Asundi, “Real-time cure monitoring of smart composite material using extrinsic Fabry-Perot interferometer and fiber Bragg grating sensors,” *Smart Material and Structures*, vol. 11, no. 2, pp. 249−255, 2002.

[7] C. Boulet, M. Hathaway, and D. A. Jackson, “Fiber-optic-based absolute displacement sensor at 1500 nm by means of channeled spectrum signal recovery,” *Optics Letters*, vol. 29, no. 14, pp. 1602−1604, 2004.

[8] B. Yu, A. Wang, G. Pickrell, and J. Xu, “Tunable-optical-filter-based white-light interferometry for sensing,” *Optics Letters*, vol. 30, no. 12, pp. 1452−1454, 2005.

[9] Y. Jiang, “High-resolution interrogation technique for fiber optic extrinsic Fabry-Perot interferometric sensors by peak-to-peak method,” *Applied Optics*, vol. 47, no. 6, pp. 925−932, 2008.

[10] V. Bhatia, M.B. Sen, K.A. Murphy, and R.O. Claus, "Wavelength-tracked white light interferometry for highly sensitive strain and temperature measurements," *Electron. Lett.*, vol. 32, no. 3, pp. 247−249, 1996.

[11] Y. J. Rao, Z. L. Ran, X. Liao, and H. Y. Deng, "Hybrid LPFG/MEFPI sensor for simultaneous measurement of high-temperature and strain," *Optics Express*, vol. 15, no. 22, pp. 14936−14941, 2007.

[12] Y. J. Rao, X. J. Wang, T. Zhu, and C. X. Zhou, "Demodulation algorithm for spatial-frequency-division-mutiplexed fiber-optic Fizeau strain sensor network," *Optics Letters*, vol. 31, no. 6, pp. 700−702, 2006.

[13] T. Liu and G.F. Fernado, "A frequency division multiplexed low-finesse finer optic Fabry-Perot sensor system for strain and displacement measurements," *Review of Scientific Instruments*, vol. 71, no. 3, pp. 1275−1278, 2000.

[14] B. Qi, G. R. Pickrell, P. Zhang, *et al*., "Novel data processing techniques for dispersive white light interferometer," *Optical Engineering*, vol. 42, no. 11, pp. 3165−3171, 2003.

[15] Y. Jiang, and C. J. Tang, "High-finesse micro-lens fiber-optic extrinsic Fabry-Perot interferometric sensors," *Smart Materials and Structures*, vol. 17, no. 5, pp. 055013, 2008.

[16] Y. Jiang and C. J. Tang, "High-finesse micro-lens optical fiber Fabry-Perot filters, " *Microwave and Optics Technology Letters*, vol. 50, no. 9, pp. 2386−2389, 2008.

[17] Y. Jiang, "Fourier transform white-light interferometry for the measurement of fiber optic extrinsic Fabry-Perot interferometric sensors," *IEEE Photo Technology Letters*, vol. 30, no. 2, pp. 75−77, 2008.

[18] Y. Jiang and C. J. Tang, "High-resolution interrogation technique for the measurement of extrinsic Fabry-Perot interferometer (EFPI) using a compensating EFPI," *Measurement Science Technology*, vol. 19, no. 6, pp. 065304, 2008.

[19] Y. Jiang and C. J. Tang, "Fourier transform white-light interferometry based spatial frequency-division multiplexing of extrinsic Fabry-Perot interferometric sensors," *Review of Scientific Instruments*, vol. 79, no. 10, pp. 106105, 2008.

[20] Y. Jiang, "Wavelength-scanning white-light interferometry with a 3 × 3 coupler-based interferometer," *Optics Letters*, vol. 33, no. 16, pp. 1869−1871, 2008.

[21] Y. Jiang, Y. Xu, and C. K. Y. Leung, "3 × 3 coupler based Mach-Zehnder interferometer and its application in the delamination detection in FRP composite," *Journal of Intelligent Material Systems and Structures*, vol. 19, no. 4, pp. 497−507, 2008.

[22] Y. Jiang, "Stabilized 3 × 3 coupler based interferometer for the demodulation of fiber Bragg grating sensors," *Optical Engineering*, vol. 47, no. 1, pp. 015006, 2008.

[23] Y. Jiang, "Four-element fiber Bragg grating acceleration sensor array," *Optics and Lasers in Engineering*, vol. 46, no. 9, pp. 695−703, 2008.

[24] Y. Jiang and C. J. Tang, "Hybrid interrogation system for intensity-type sensor/fiber Bragg grating/extrinsic Fabry-Perot interferometer," *Measurement Science and Technology*, vol. 20, pp. 025308, 2009,.

[25] Y. Jiang, C. J. Tang, and F. J. Zhang, "WDM/SDM of intensity-type fiber-optic sensors," *Microwave and Optics Technology Letters*, vol. 51, no. 2, pp. 432−435, 2009.